International Journal of Engineering Research & Technology (IJERT)
ISSN: 2278-0181
Vol. 2 Issue 10, October - 2013

# Selective Synthesis of 2-Aryl-1-arylmethyl-1*H*-benzimidazoles Using Carbon doped $MoO_3$ as an Efficient Heterogeneous Catalyst

Madhukar E. Navgire [*a] and Machhindra K. Lande [b]

[a]*Department of Chemistry, *Jijamata College of Science and Arts, Bhende, Newasa, Ahmednagar, India, PIN 414605*
[b]*Department of Chemistry, Dr. Babasaheb Ambedkar Marathwada University, Aurangabad 431004, India*

## Abstract

*A series of carbon doped $MoO_3$ as catalyst were prepared by simple impregnation method. The carbon source was prepared from the Acacia Arabica plant wood. The effect of addition of carbon composite on the structure, particle size and morphology was investigated successfully. The prepared materials were tested for catalytic activities for the synthesis of 2-Aryl-1-arylmethyl-1H-benzimidazole derivatives using o-phenylenediamines with aromatic aldehydes (1:2 molar ratios) in EtOH:$H_2O$ under refluxed condition. The catalytic acti4vity increases with increase in carbon wt % loading. This new method consistently has the advantage of excellent yields, short reaction times and environmentally benign..*



## 1. Introduction

Acid-catalyzed organic reactions are numerous and the usage of solid acid catalysts is very important in several industrial and environmental processes [1-6]. The use of conventional liquid acids and Lewis acids has significant risks in handling, containment, disposal and regeneration due to their toxic and corrosive nature. Hence, there is a need for the development of strong solid acid catalysts which must be stable, regenerable and active at moderate temperatures. In recent years, inorganic solid acid-catalyzed organic transformations are gaining much attention due to proven advantage of heterogeneous catalysts, like easy product isolation, mild reaction conditions, high selectivity, and ease in recovery and recyclability of the catalysts and substantial reduction in the generation of waste materials [7-9]. Various solid acids such as zeolites, mesoporous materials, supported and unsupported metal oxides have been used as catalysts for variety of reactions like alkylation, oxidation, condensation, isomerization, etc. [10]. Interestingly, molybdenum oxide exhibits excellent activity for a wide range of organic synthetic and transformation reactions. It has been receiving much attention, amongst other solid acid catalysts, due to its superior catalytic activity which possesses both strong Lewis and Bronsted acidity [11, 12]. Supported $MoO_3$ has been found to be highly active in various acid catalyzed reactions [13-18].

Interest in benzimidazole-containing structures stems from their widespread occurrence in molecules that exhibit significant activity against several viruses such as HIV, herpes (HSV-1), RNA, influenza and human cytomegalovirus (HCMV) [19]. Substituted benzimidazole derivatives have found commercial applications in veterinarian medicine as anthelmintic agents and in diverse human therapeutic areas such as treatment of ulcers and as antihistamines [20, 21]. The traditional synthesis of benzimidazoles involves the reaction between o-phenylenediamine and a carboxylic acid or its derivatives (nitriles, amidates, orthoesters) under harsh dehydrating conditions [22]. Benzimidazoles have also been prepared on solid-phase to provide a combinatorial approach [23]. However, many of these methods have several drawbacks such as low yields, use of expensive reagents, and a special oxidation process or long reaction times, tedious work-up procedures, co-occurrence of several side reactions and poor selectivity. Therefore, the search continues for a better catalyst for the synthesis of 2-Aryl-1-arylmethyl-1H-benzimidazoles in terms of operational simplicity, economic viability and in particular, with greater selectivity.

Thus taking into considerations of above points, the present article report the improvement in structural and catalytic properties of $MoO_3$ by addition of carbon. The carbon substrate was prepared and utilized from natural sources like *Acacia Arabica* plant. A series of carbon-doped $MoO_3$ nanocomposite materials were prepared by conventional standard impregnation method. The catalyst was then tested on the synthesis of 2-Aryl-1-arylmethyl-1H-benzimidazole derivatives Scheme 1.

## 2. Results and Discussion

### *2.1. XRD analysis*

X-ray diffraction results show the crystal structures, phases and lattice modification of the pure $MoO_3$ and the Carbon doped $MoO_3$ composite namely CMP-1, CMP-2 and CMP-3 samples shown in Figure 1. All the samples shows number of XRD peaks, positioned at 2θ(degree) = 23.3, 27.3, 29.5, 33.7 38.9, 45.9, 49.3, 52.8, 64.8 and 72.9, indicating hkl values due to planes (110), (021), (040), (111), (060), (210), (002), (240), (190) and (212), that can be easily indexed as orthorhombic $MoO_3$ in the Joint Committee on Powder Diffraction Standards (JCPDS) database card No. 76-1003 [24]. The orthorhombic crystal structure with lattice parameter a=3.9628Å, b=13.8550Å and c=3.6964Å. The strong and sharp peaks suggest that as-prepared materials are highly crystalline. An XRD technique fails to recognize the peaks due to carbon sample due to its less crystalline nature as compared $MoO_3$. Due to addition of 3 wt% carbon in $MoO_3$ with PEG-400 (CMP-0) as a surfactant, it was interestingly noted that the high intensity peak observed at 29.5 (2θ° for hkl 040).

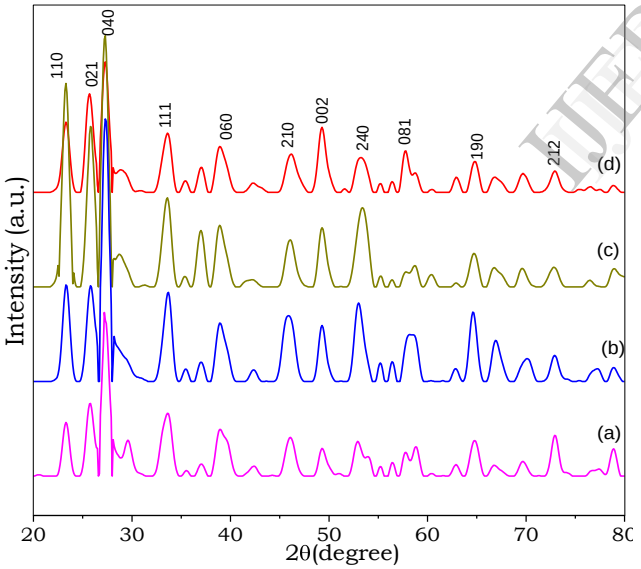


***Figure 1**: XRD patterns of a) CPM-0, b) CPM-1, c) CPM-2, d) CPM-3*

Generally, the average particle size of solid materials can be estimated from X-ray line broadening and full width half maximum (FWHM) values using Debye-Scherrer equation [25].

$\theta = K\lambda/\beta\cos\theta$

Where, τ= Particle size, K= shape factor (0.94), λ= x-ray wavelength (1.5432 Å), θ= Bragg diffraction angle, β= line broadening at FWHM (full width half maximum). The particle sizes of prepared catalysts with different carbon wt % doped $MoO_3$ are shown in Table 1. It indicates that the minimum particle size (18.46 nm) and crystallite size from XRD peaks (09.76 nm) were found for the 3wt % carbon loading on $MoO_3$.

**Table 1:** Estimation of Particle size of series of catalyst

| **Entry** | **Carbon loading** (in wt %) | **FWHM** | **Crystallite size** (in nm) | **Particle size** (τ in nm) |
|---|---|---|---|---|
| 1 | 0wt% (CMP-0) | 0.8782 | 09.82 | 18.576 |
| 2 | 1wt% (CMP-1) | 0.8524 | 10.40 | 19.156 |
| 3 | 2wt% (CMP-2) | 0.8235 | 08.18 | 19.817 |
| 4 | 3wt% (CMP-3) | 0.8839 | 09.76 | 18.467 |

***Figure 2**: The SEM image of a) and b) for CMP-0, c) and d) for CMP-3*

### *2.2 SEM and EDS analysis*

To study the surface topography and elemental composition, the SEM with EDS was investigated systematically. Figure 2 shows the variation in morphology of $MoO_3$ samples with carbon addition. Figure 2(a and b) shows morphology of pure $MoO_3$ (CMP-0) that is crystalline in nature. It can be seen from figure 2(c and d) that the samples CMP-3 shows decrease in the particle size and development of porous surface. From the SEM micrograph, the effect of addition of carbon clearly shows alteration in particle size and morphology with increasing porosity.

Elemental compositions of 3 wt% carbon doped $MoO_3$ were represented in Figure 3. The observed Mo: C: O atomic ratios 9.58: 34.51: 55.91 respectively, are fairly close to the expected bulk ratios indicating uniform distribution of the metal species inside the samples. It was supports that, the minimum stoichiometric ratio of desired elements in the CMP-3 is maintained.

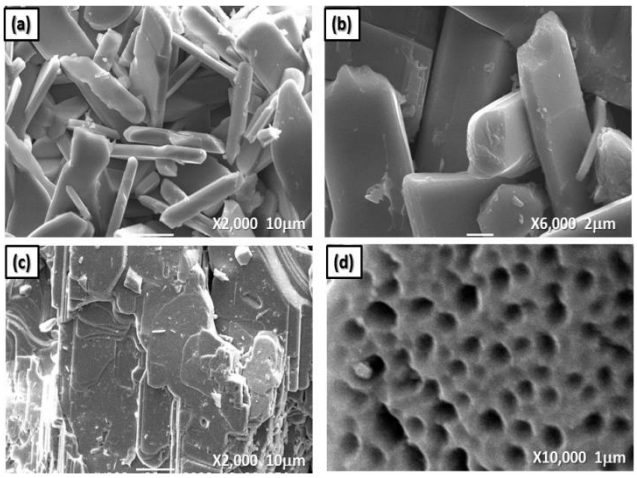

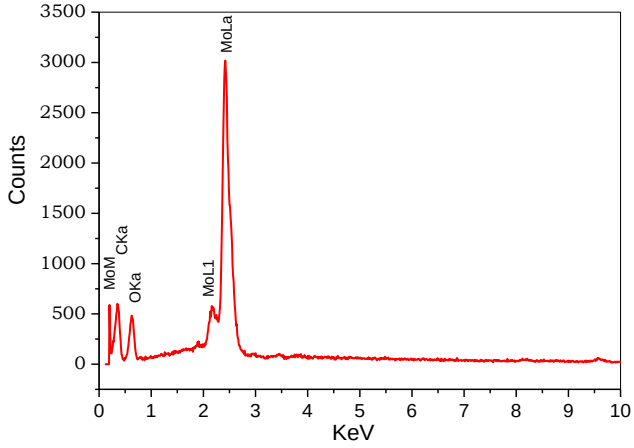


***Figure 3**. EDS Spectrum of CMP-3*

### *2.3 FT-IR analysis*

Figure 4 (a) shows the FT-IR spectra of CMP-0 (pure $MoO_3$). A band at 877 $cm^{-1}$ is characteristic of terminal molybdenum oxygen double bond (Mo=O). The bands at 1416 and 1562 $cm^{-1}$ were attributed due to C-C and C=C vibrations [26]. The broad band around 3417 $cm^{-1}$ is due to O-H stretching vibration modes of the adsorbed water on the surface of the powder [27]. The Figure 4 (b-d) shows the FT-IR spectra of CMP-1, CMP-2 and CMP-3 respectively. A sharp band appears in the range 867-866 $cm^{-1}$ is due to the terminal Molybdenum=Oxygen double bond (Mo=O). The bands at 1416 -1600 $cm^{-1}$ were attributed due to C-C and C=C vibrations, the additional band around 2924 $cm^{-1}$ probably may due to $CH_2$ and or C (OH) stretching mode. While broad band around 3350-3398 $cm^{-1}$ is due to O-H stretching vibration modes of the adsorbed water [28].

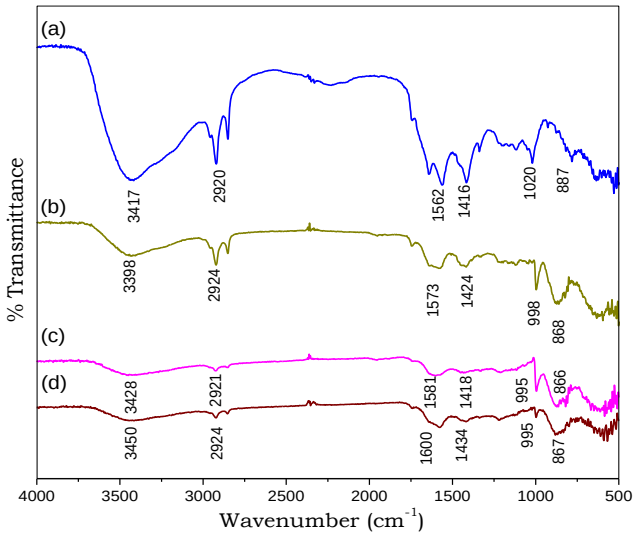


***Figure 4:** FT-IR spectrum of a) CMP-0, b) CMP-1, c) CMP-2, d) CMP-3,*

### *2.4 TEM analysis*

The TEM images shown in Figure 5 indicate the obtained nano-sized particles have clarity. The TEM images of pure $MoO_3$ in Figure 5 (a) shows the presence of highly crystalline nano rods of $MoO_3$ with particle size varying in between 15 to 20 nm in width which is matching with XRD analysis. From Figure 5 (b and c) for CMP-3, it was seen that the decrease in average particle size of modified sample in the range of 10 to 18 nm. From the images, it is clearly seen that addition of carbon on $MoO_3$ surface improves the catalytic activity. From the selected area diffraction patterns (SEAD) shown in Figure 6 (d), supports the (110), (040), and (021) surfaces of the orthorhombic form of $MoO_3$.

### *2.5 BET Surface area*

The $N_2$-BET surface area of 3 wt.% carbon doped $MoO_3$ samples are shown in Figure 6. The amount of $N_2$ gas adsorbed-desorbed at a given pressure allows determining the surface area of material. The isotherm indicates large volume was adsorbed on surface of material. Single point surface area at P/Po is 2.5042 $m^2/g$ and BET Surface Area is 2.7629 $m^2/g$. It means prepared material has higher surface area. Due to this, material gives higher catalytic activity.

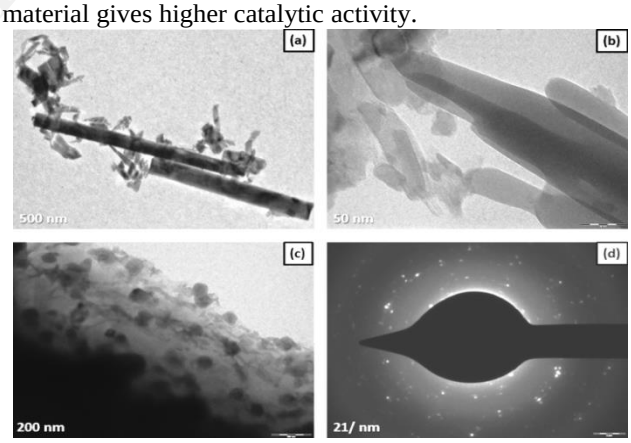


***Figure 5** TEM images of a) CMP-0, b) and c) CMP-3, d) SEAD patterns of CMP-3*

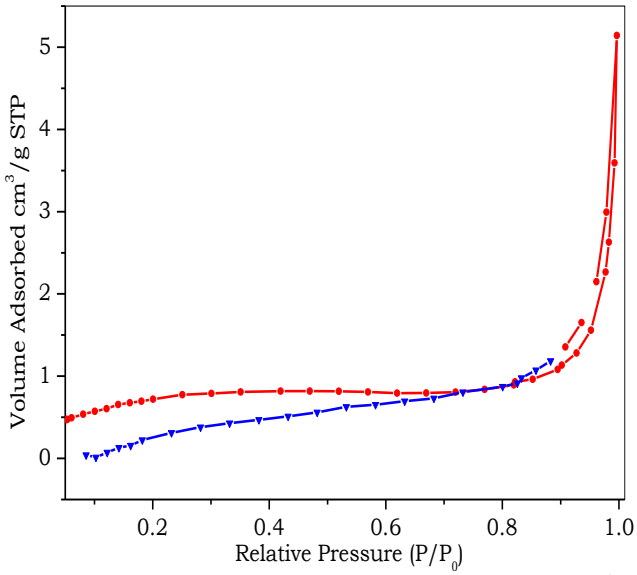


***Figure 6*** *$N_2$ adsorption-desorption isotherms of CMP-3*

### *2.6 TPD measurement*

The $NH_3$-TPD desorption data provides information about the total concentration and strength of acidic sites present in the synthesized material [29]. The $NH_3$-TPD analysis of CMP-3 solid heterogeneous catalyst is shown in **Figure 7**. A broad ammonia desorption profile in the 500–600°C range with highest desorption around 520°C could be noted. This broad peak can be considered as an indication for the presence of high concentration of acid sites with moderate strength. In addition to this broad peak, two low temperature desorption peaks are also observed at 248°C and 448°C respectively. From the analytical data, it was observed that during experiment $NH_3$-desorbed at three different temperature regions such as 200–350, 380–480 and 500–600°C. These are normally attributed to $NH_3$ chemisorbed on weak, medium and strong acid sites, respectively. At 248°C temperature region 0.01539 mmol/gm of $NH_3$ was desorbed which confirms presence of Lewis acidic sites. At 448°C and 520°C region 0.02006 mmol/gm and 0.10176 mmol/gm of $NH_3$ was desorbed which confirms the presence of Bronsted acidic sites. Hence, the total strength of the acidic sites present in synthesized CMP-3 catalytic material was found 0.13721 mmol/gm. It means the material is more suitable for organic transformation reactions.

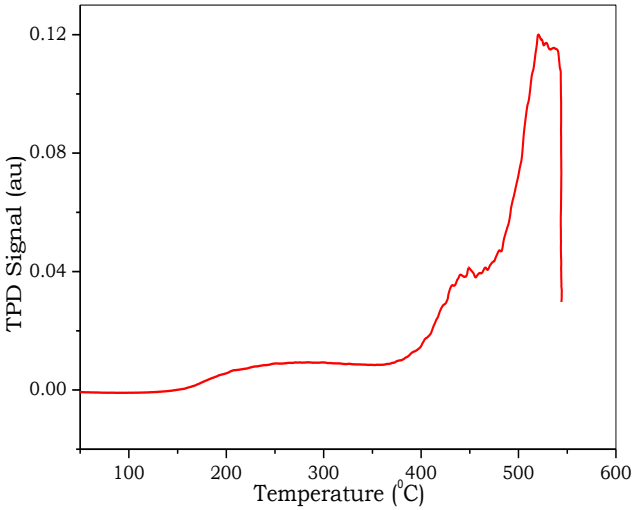


***Figure 7*** *$NH_3$-TPD measurement of CMP-3*

### *2.7 Catalytic Activity results*

In order to get test the role of synthesized catalytic material, we have carried out the model reaction of o-phenylenediamine and benzaldehyde in presence of carbon-doped $MoO_3$ (0.1 g) by refluxing in Ethanol: Water (2:1), and also in various solvents, such as water. Methanol, acetonitrile, tetrahydrofuran, ethanol and ethanol: water; to examine the solvent effect from this study, it has been observed that ethanol: water (2:1) in the best solvent medium to carry out the synthesis of desired compounds. After optimization of solvent effect we also studied optimized the amount of catalyst. Interestingly, it was observed that different wt % (0, 1, and 2) of CMP furnishes the moderate amount of yields of the products (Table 2, entry 8-10). The CMP-3 catalytic material shows maximum yield about 89%.

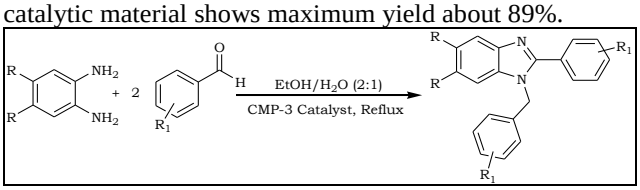


**Scheme 1**

To test the generality of this reaction, a series of aromatic aldehydes and o-phenylenediamines were subjected to the optimal reaction conditions. Almost all substrates could give their corresponding 1,2-disubstituted benzimidazoles exclusively as a single product. The results are documented in Table 3. Therefore, under optimized conditions, the method was further employed to synthesize variety of 2-Aryl-1-arylmethyl-1*H*-benzimidazoles and found that electron withdrawing and donating aldehydes reacts without any

significant loss in activity to give the desired products in good yields (Table 3 entry 3a-3g).

The catalyst was recovered by filtration of reaction mixture under hot condition. The recovered catalyst was washed several times with acetone and dried at 100°C. The separated catalyst was again reused for the fresh reaction. In these cases the yield of product is found to be 89, 89, 88 and 88% in successive time use. Thus, the activity of catalyst was found to be diminished to same extent after several runs.

**Table 2:** Comparative study of synthesis of benzimidazole with different catalyst and solvent

| Entry | Catalyst | Solvent | Time (Minute) | Yield (%)[a] |
|---|---|---|---|---|
| 1 | CMP-3 | $H_20$ | 180 | 65 |
| 2 | CMP-3 | EtOH | 150 | 85 |
| 3 | CMP-3 | MeOH | 210 | 82 |
| 4 | CMP-3 | MeCN | 240 | 63 |
| 5 | CMP-3 | THF | 240 | 60 |
| 6 | CMP-3 | EtOH:$H_20$ (1:1) | 120 | 84 |
| 7 | **CMP-3** | **EtOH:$H_20$ (2:1)** | **120** | **89** |
| 8 | CMP-0 | EtOH:$H_20$ (2:1) | 120 | 72 |
| 9 | CMP-1 | EtOH:$H_20$ (2:1) | 120 | 81 |
| 10 | CMP-2 | EtOH:$H_20$ (2:1) | 120 | 86 |

**Reaction conditions:** *o*-phenylenediamine (1 mmol), benzaldehyde (2 mmol) and 0.1 g catalyst and EtOH: $H_2O$ (2:1) under reflux condition. [a]Isolated Yield.

**Table 3.** Synthesis of benzimidazole derivatives

| Entry | R | $R_1$ | Time (Minute) | Yield (%)[a] | Melting Point (°C) | |
|---|---|---|---|---|---|---|
| | | | | | Observed | Literature |
| 3a | H | H | 120 | 89(89,88, 88)[b] | 130 | 132 [30] |
| 3b | H | 2-Cl | 150 | 85 | 160 | 157-159 [31] |
| 3c | H | 4-F | 210 | 82 | 113 | 111-114 [30] |
| 3d | H | 3-$NO_2$ | 240 | 63 | | - |
| 3e | H | 4-Br | 240 | 60 | 159 | 157-158 [30] |
| 3f | H | 4-Cl | 120 | 84 | 135 | 135-136 [30] |
| 3g | $CH_3$ | 2-Cl | 120 | 89 | | - |

**Reaction conditions:** *o*-phenylenediamine (1 mmol), benzaldehydes (2 mmol) and 0.1 g CMP-3 catalyst and EtOH: $H_2O$ (2:1) solvent under reflux condition. [a]Isolated Yield, [b]After consecutive run.

The synthetic protocol described herein allows exclusively biologically significant benzimidazoles under the heterogeneous catalysis using carbon-doped $MoO_3$ as a catalyst. This synthetic procedure offers several advantages including mild reaction conditions, greater selectivity, high product yields as well as simple experimental and isolation procedure, which makes it useful and attractive process for large scale synthesis of these compounds.

## 3. Experimental Section

### *3.1 Procedure for the Carbon-doped $MoO_3$ catalysts*

The carbon was prepared from *Acacia Arabica* plant as a natural source. In the first step dried wood burnt in absence of air, then resulting charcoal was crushed into fine powder. Finally, the obtained powder material was calcined at 500°C. Carbon-doped $MoO_3$ catalysts were prepared by conventional standard impregnation method. To impregnate carbon-doped $MoO_3$, the solution was obtained by dissolving ammonium heptamolybdate (0.2M) in deionized water. The system was kept under constant stirring and sustaining the pH = 8 by simultaneous addition of oxalic acid (0.2M) and 1:1 $NH_4OH$. The fine powdered carbon was added with 0 wt% (CMP-0), 1 wt% (CMP-1), 2 wt% (CMP-2) and 3 wt% (CMP-3) respectively. Then PEG-400 (0.5M) was added as a surfactant. The excess water was evaporated on the water bath with continuous stirring. The resultant precursor was then dried at 110°C for 12 h and then finally calcined at 500°C for 2 h in an air atmosphere.

### *3.2 Characterization of material*

X-ray diffraction analyses (XRD) of the prepared catalyst were performed using a Philips X-ray diffractometer. The wavelength used for the XRD analysis was 1.540 Å with radiation of CuKα. The diffracting angle (θ) was varied in between 20–80. The Scanning electron microscopy with energy dispersive spectroscopy (SEM-EDS) characterization was conducted using a JEOL JED 2300 (LA) instrument. The Fourier transformation infra-red spectra (FT-IR) were recorded on FT-IR spectrometer JASCO-FTIR/4100 Japan, using dry KBr as standard reference in the range of 4000-600 $cm^{-1}$. The microscopic nanostructure and particle size were determined using a CM-200 PHILIPS transmission electron microscope (TEM) at 200 kV ($L$ =600, λ= 0.0025 nm). The surface area of samples was characterized by the BET method performing adsorption of nitrogen at 77 K with the apparatus Micromeritics ASAP 2010. Temperature programmed desorption ($NH_3$-TPD) measurements were carried out on a Micrometrics Instrument corporation Chemisoft TPx V1.02 unit 1 (2750). All products are known compounds and their physical data, FT-IR;$^1$H NMR and mass spectra were essentially identical with those of authentic samples. Thin layer chromatography was performed on Merck-precoated silica gel 60-F254 plates. $^1$HNMR spectra were recorded on 300 MHz in $CDCl_3$ as solvent and

chemical shifts values are recorded in ppm relative to tetramethylsilane (TMS) as an internal standard. MS spectra were taken by Shimadzu QP1100EX Mass Spectrometer operating at an ionization potential of 70eV.

***3.3 Procedure for the synthesis of substituted 2-aryl-1-arylmethyl-1H-benzimidazoles***

A mixture of aromatic aldehydes (2 mmol), o-phenylenediamines (1 mmol) in the presence of carbon-doped $MoO_3$ (0.1 g) was refluxed in Ethanol: Water (2:1) for the time mentioned in **Table 3**. The progress of the reaction was monitored by TLC using pet ether: ethyl acetate as a solvent system. After completion of the reaction, the reaction mass was filtered, and the filtrate was concentrated under reduced pressure, the crude product obtained was recrystallized from ethanol to afford pure products.

***3.4 Physical and Spectroscopic data***

**1-benzyl-2-phenyl-1H-benzo[d]imidazole (a):** $^1$HNMR ($CDCl_3$, 300MHz) δ: 8.15-7.15 (m, 10H), 6.58 (dd, 2H), 6.25 (dd, 2H), 5.45 (s, 2H); IR (ν*max.*; KBr, $cm^{-1}$): 3059, 1599, 1489, 1394 740; Mass: m/z 284.

**1-(2-chlorobenzyl)-2-(2-chlorophenyl)-1H-benzo[d]imidazole (b):** $^1$HNMR ($CDCl_3$, 300MHz) δ: 7.55-7.25 (m, 8H), 7.06 (d, 2H), 6.65 (dd, 2H), 5.38 (s, 2H); IR (ν*max.*; KBr, $cm^{-1}$): 3059, 1591, 1442, 1400, 746, 727.

**1-(4-fluorobenzyl)-2-(4-fluorophenyl)-1H-benzo[d]imidazole (c):** $^1$HNMR ($CDCl_3$, 300MHz) δ: 7.65 (m, 2H), 7.58-7.46 (m, 4H), 7.28-7.15 (m, 4H), 6.95 (dd, 2H), 5.41 (s, 2H); IR (ν*max.*; KBr,$cm^{-1}$): 3070, 1593, 1489, 1402, 744.

**1-(3-nitrobenzyl)-2-(3-nitrophenyl)-1H-benzo[d]imidazole (d):** $^1$HNMR ($CDCl_3$, 300MHz) δ: 8.85 (s, 1H), 8.52 (d, 1H), 8.25 (d, 1H), 8.05 (s, 1H), 7.92 (d, 1H), 7.71 (dd, 2H), 7.55 (dd, 1H); 7.45-7.25 (m, 4H), 5.61 (s, 2H); IR (ν*max.*; KBr,$cm^{-1}$): 3055, 1521, 1475, 1315, 752.

**1-(4-bromobenzyl)-2-(4-bromophenyl)-1H-benzo[d]imidazole (e):** $^1$HNMR ($CDCl_3$, 300MHz) δ: 7.92 (m, 2H), 7.65-7.42 (m, 4H), 7.38-7.21 (m, 4H); 6.95 (m, 2H), 5.40 (s, 2H); IR (ν*max.*; KBr,$cm^{-1}$): 3076, 1506, 1479, 748, 609.

**1-(4-chlorobenzyl)-2-(4-chlorophenyl)-1H-benzo[d]imidazole (f):** $^1$HNMR ($CDCl_3$, 300MHz) δ: 7.92 (m, 2H), 7.85 (m, 2H), 7.62 (m, 2H), 7.45 (m, 2H), 7.25 (m, 2H), 7.02 (m, 2H), 5.45 (s, 2H); IR (ν*max.*; KBr, $cm^{-1}$): 3053, 1600, 1429, 831, 744.

**1-(2-chlorobenzyl)-2-(2-chlorophenyl)-5-methyl-1H-benzo[d]imidazole (g):** $^1$HNMR ($CDCl_3$, 300MHz) δ: 8.10 (s, 1H), 7.70 (m, 1H), 7.6-7.45 (m, 4H), 7.40-7.15 (m, 4H), 7.05 (dd, 1H), 5.45 (s, 2H), 2.45 (s, 3H); IR (ν*max.*; KBr, $cm^{-1}$): 3059, 1537, 1452, 1365, 800, 709.

**4. Conclusions**

In summary the present paper describes a new, efficient and eco-friendly route for the synthesis of 2-Aryl-1-arylmethyl-1*H*-benzimidazoles. The 3 wt % carbon doped $MoO_3$ (CMP-3) catalyst exhibits excellent catalytic activity for the condensation of various aromatic aldehydes and o-phenylenediamines. Most importantly, this catalyst facilitates the reaction under refluxing conditions providing supports in the reaction, enhances the reaction rate and thereby the excellent yields of the products. We have also compared the time required and product yields for the synthesis of benzimidazole by the addition of amount of carbon in $MoO_3$. The catalyst can be prepared with easily available and from inexpensive reagents by simple impregnation method. The prepared catalyst is reusable and non-hazardous. A simple procedure combined with low toxicity and reusability of the catalysts, provides an economic and waste-free chemical method for the synthesis of 2-Aryl-1-arylmethyl-1*H*-benzimidazoles.

**Acknowledgments**

The authors are grateful to the Head, Department of Chemistry, Dr. Babasaheb Ambedkar Marathwada University, Aurangabad, India, and Principal, Jijamata College of Science and Arts, Bhende, Newasa, Ahmednagar for providing the all required facilities to carry out the work.



## References

1. Corma, A; Garcia, H. Lewis Acids: From Conventional Homogeneous to Green Homogeneous and Heterogeneous Catalysis. *Chem. Rev*. **2003**, 103, 4307-4366.
2. Kappe, C; Stadler, A. Biginelli Dihydropyrimidine Synthesis. *Org. React*. **2004**, 63,1.
3. Stefane, B. Selective Addition of Organolithium Reagents to $BF_2$-Chelates of *β*-Ketoesters. *Org. Lett*. **2010**, 12, 2900.
4. Guillena, G; Raman, D. J.; Yus, M. Hydrogen Autotransfer in the N-Alkylation of Amines and Related Compounds using Alcohols and Amines as Electrophiles. *Chem. Rev*. **2010**, 110, 1611-1641.
5. Kamata, K.; Ishimoto, R.; Hirano, T.; Kuzuya, S.; Uehara, Mizuno, K.N. Epoxidation of Alkenes with Hydrogen Peroxide Catalyzed by Selenium-Containing Dinuclear Peroxotungstate and Kinetic, Spectroscopic, and Theoretical Investigation of the Mechanism. *Inorg. Chem*. **2010**, 49, 2471-2478.
6. Tanabe, K; H¨olderich, W.F. Industrial application of solid acid–base catalysts. *Appl. Catal. A* 1999, 181, 399-434.

7. Clark, J.H. Solid Acids for Green Chemistry. *Acc. Chem. Res*. **2002**, 35, 791-797.
8. Corma, A. Inorganic Solid Acids and Their Use in Acid-Catalyzed Hydrocarbon Reactions. *Chem. Rev*. **1995**, 95,559-614.
9. Okuhara, T. Water-Tolerant Solid Acid Catalysts. *Chem. Rev*. **2002**, 102, 3641-3666.
10. Mitsutani, A. Future possibilities of recently commercialized acid/base-catalyzed chemical processes. *Catal. Today* **2002**, 73, 57-63.
11. Baig, A; Ng, F.T.T. A Single-Step Solid Acid-Catalyzed Process for the Production of Biodiesel from High Free Fatty Acid Feedstocks. *Energy Fuels* 2010, 24, 4712-4720.
12. de Paiva, Jr.J.B; Monteiro, W.R; Zacharias, M.A; Rodrigues, J.A.J; Cortez, G.G. Characterization and catalytic behavior of $MoO_3/V_2O_5/Nb_2O_5$ systems in isopropanol decomposition. *Braz. J. Chem. Eng*. 2006, 23, 517-524.
13. Letti, L; Ramis, G; Busca, G; Bregani, F; Forzetti, P. Characterization and reactivity of $MoO_3/SiO_2$ catalysts in the selective catalytic oxidation of ammonia to $N_2$. *Catal. Today* 2000, 61, 187-195.
14. Dongare, M.K; Patil, P.T; Malshe, K.S. US Patent 6 (2004) 791,000.
15. Radwan, N.R.E; El-Shobaky, H.G; El-Molla, S.A. Surface and catalytic properties of pure $CeO_2$ and $MoO_3$-doped $NiO/TiO_2$ system. *Appl. Catal. A* 2006, 297, 31-39.
16. Dongare, M.K; Bhagvat, V.V; Ramana, C.V; Gurjar, M.K. Silica supported $MoO_3$: a mild heterogeneous catalyst for the Beckmann rearrangement and its application to some sugar derived ketoximes. *Tetrahedron Lett*. **2004**, 45, 4759-4762.
17. Lande, M.K; Navgire, M.E; Rathod, S.B; Katkar, S.S; Yelwande, A.A; Arbad B.R. An efficient green synthesis of quinoxaline derivatives using carbon-doped $MoO_3$–$TiO_2$ as a heterogeneous catalyst. *J. Ind. Eng. Chem*. **2012**, 18, 277-282.
18. Rathod, S.B; Lande, M.K; Arbad, B.R. Synthesis, Characterization and Catalytic Application of $MoO_3/CeO_2$-$ZrO_2$ Solid Heterogeneous Catalyst for the Synthesis of Benzimidazole Derivatives. *Bull. Korean Chem. Soc*. **2010**, 31, 2835-2840.
19. (a) Tebbe, M.J; Spitzer, W.A; Victor, F; Miller, S.C; Lee, C.C; Sattelberg, T.R; Mckinney, E; Tang, C.J. Antirhino/Enteroviral Vinylacetylene Benzimidazoles: A Study of Their Activity and Oral Plasma Levels in Mice. *J. Med. Chem*. **1997**, 40, 3937-3946. (b) Porcari, A.R; Devivar, R.V; Kucera, L.S; Drach, J.C; Townsend, L.B. Design, Synthesis, and Antiviral Evaluations of 1-(Substituted benzyl)-2-substituted-5,6-dichlorobenzimidazoles as Nonnucleoside Analogues of 2,5,6-Trichloro-1-(β-d-ribofuranosyl) benzimidazole. *J. Med. Chem*. **1998**, 41, 1252-1262. (c) Roth, M; Morningstar, M.L; Boyer, P.L; Hughes, S.H; Bukheit, R.W; Michejda, C.J. Synthesis and Biological Activity of Novel Nonnucleoside Inhibitors of HIV-1 Reverse Transcriptase. 2-Aryl-Substituted Benzimidazoles. *J. Med. Chem*. **1997**, 40, 4199-4207. (d) Migawa, M.T; Giradet, J.L; Walker, J.A; Koszalka, G.W; Chamberlain, S.D; Drach, J.C; Townsend, L.B. Design, Synthesis, and Antiviral Activity of α-Nucleosides: d- and l-Isomers of Lyxofuranosyl- and (5-Deoxylyxofuranosyl)benzimidazoles. *J. Med. Chem*. **1998**, 41, 1242-1251.
20. Spasov, A.A; Yozhitsa, I.N; Bugaeva, L.I; Anisimova, V.A; Benzimidazole derivatives: Spectrum of pharmacological activity and toxicological properties (a review). *Pharm. Chem. J*. **1999**, 33, 232-243.
21. Mason, J.S; Morize, I; Menard, P.R; Cheney, D.L; Hume, C; Labaudiniere, R.F. New 4-Point Pharmacophore Method for Molecular Similarity and Diversity Applications: Overview of the Method and Applications, Including a Novel Approach to the Design of Combinatorial Libraries Containing Privileged Substructures. *J. Med. Chem*. **1999**, 42, 3251-3264.
22. Dudd, L.M; Venardou, E; Garcia-Verdugo, E; Licence, P; Blake, A.J; Wilson, C; Poliakoff, M. Synthesis of benzimidazoles in high-temperature water. *Green Chem*. **2003**, 5, 187-192.
23. Reddy, B.M; Chaudhry, B; Reddy, E; Fernandez, A; Characterization of $MoO_3/TiO_2$–$ZrO_2$ catalysts by XPS and other techniques. *J. Mol. Catal. A* **2000**, 162, 431-441.
24. Kihlborg, L. Ark. Kemi. **1963**, 21, 557.
25. Taylor, X-ray Metallography John Wiley, New York, **1961**, 678.
26. Oyama, S.T; Radhakrishnan, S; Seman, M; Kondo, J.N; Domen, K; Asakura, K. Control of Reactivity in C−H Bond Breaking Reactions on Oxide Catalysts: Methanol Oxidation on Supported Molybdenum Oxide. *J. Phys. Chem.* **2003**, 107, 1845-1852.
27. Ganguly; A; George, R. Synthesis, characterization and gas sensitivity of $MoO_3$ nanoparticles. *Bull. Mater. Sci*. **2007**, 30, 183-186.
28. Cheng, T; Fang, Z; Zou, G; Hu, Q; Hu, B; Yang, X; Zhang, Y. A one-step single source route to carbon nanotubes. *Bull. Mater. Sci*. **2006**, 29, 701-704.
29. Luo, H; Wei, M; Wei, K; A new metastable phase

of crystallized $MoO_3 \cdot 0.3H_2O$ nanobelts. *Mater. Chem. Phys.* **2009**, 113, 85-90.
30. Auroux, A; Gervasini, A.Microcalorimetric study of the acidity and basicity of metal oxide surfaces. *J. Phys. Chem.*, **1990**, 94, 6371-6379.
31. Kawai, M; Tsukuda, M; Tamaru, K. Surface electronic structure of binary metal oxide catalyst $ZrO_2/SiO_2$. *Surf. Sci.*, **1981**, 111, L716-L720.